Large β-Delayed One and Two Neutron Emission Rates in the Decay of ^{86}Ga

K. Miernik,[1,2,*] K. P. Rykaczewski,[1] C. J. Gross,[1] R. Grzywacz,[1,3] M. Madurga,[3] D. Miller,[3] J. C. Batchelder,[4] I. N. Borzov,[1,5] N. T. Brewer,[3,6] C. Jost,[3] A. Korgul,[2] C. Mazzocchi,[2] A. J. Mendez II,[1] Y. Liu,[1] S. V. Paulauskas,[3] D. W. Stracener,[1] J. A. Winger,[7] M. Wolińska-Cichocka,[1,4,8] and E. F. Zganjar[9]

[1]*Physics Division, Oak Ridge National Laboratory, Oak Ridge, Tennessee 37830, USA*
[2]*Faculty of Physics, University of Warsaw, Warsaw PL-00-681, Poland*
[3]*Department of Physics and Astronomy, University of Tennessee, Knoxville, Tennessee 37996, USA*
[4]*Oak Ridge Associated Universities, Oak Ridge, Tennessee 37831, USA*
[5]*Joint Institute for Nuclear Research, 141980 Dubna, Russia*
[6]*Department of Physics and Astronomy, Vanderbilt University, Nashville, Tennessee 37235, USA*
[7]*Department of Physics and Astronomy, Mississippi State University, Mississippi 39762, USA*
[8]*Heavy Ion Laboratory, University of Warsaw, Warsaw PL-02-093, Poland*
[9]*Department of Physics and Astronomy, Louisiana State University, Baton Rouge, Louisiana 70803, USA*

(Received 1 July 2013; published 24 September 2013)

Beta decay of ^{86}Ga was studied by means of β-neutron-γ spectroscopy. An isotopically pure ^{86}Ga beam was produced at the Holifield Radioactive Ion Beam Facility using a resonance ionization laser ion source and high-resolution electromagnetic separation. The decay of ^{86}Ga revealed a half-life of 43^{+21}_{-15} ms and large β-delayed one-neutron and two-neutron branching ratios of $P_{1n} = 60(10)\%$ and $P_{2n} = 20(10)\%$. The $\beta\gamma$ decay of ^{86}Ga populated a 527 keV transition that is interpreted as the deexcitation of the first 2^+ state in the $N = 54$ isotone ^{86}Ge and suggests a quick onset of deformation in Ge isotopes beyond $N = 50$.

DOI: 10.1103/PhysRevLett.111.132502 PACS numbers: 23.20.Lv, 23.40.−s, 26.30.Hj, 27.50.+e

Beta-delayed neutron emission from nuclei (βn) was discovered and interpreted as early as 1939 [1,2]. Today over 200 β-delayed neutron emitters are known. The process occurs whenever the β^- decay energy (Q_β) is larger than the neutron separation energy (S_n) in the daughter nucleus. It was not until 1960 that it was realized [3] that multineutron emission may appear in very neutron-rich nuclei, when Q_β is larger than the two (or more) neutron separation energy ($S_{2n,3n,...}$). Beta-delayed two-neutron emission ($\beta 2n$) was observed for the first time in 1979 by Azuma *et al.* [4] for the case of ^{11}Li. So far 17 $\beta 2n$ emitters have been experimentally found [5]. The largest reported $\beta 2n$ probability is $P_{2n} = 16(6)\%$ for ^{19}B [6]. There are only two known cases of $\beta 2n$ emitters heavier than iron, namely ^{98}Rb [7] and ^{100}Rb [8], where the reported branching ratios are rather small, 0.060(9)% and 0.16(8)%, respectively.

Nuclear models like the finite-range droplet model with quasiparticle random-phase approximation (FRDM + QRPA) [9,10] predict that in the decay of heavier neutron-rich nuclei at and beyond the current experimental limits, β-delayed multineutron emission probability may be comparable to the $\beta 1n$ decay. In fact, some of the reported $\beta 1n$ branching ratios may include undetected $\beta 2n$ emission [11]. In view of the fact that the only known $\beta 2n$ branches in heavier nuclei are very small, it is also possible that the models are systematically overpredicting the probability of $\beta 2n$ emission. So far insufficient experimental evidence exists to support or guide the theoretical models of $\beta 2n$ probabilities in heavy nuclei. These predictions affect, in particular, the astrophysical process of rapid-neutron capture (r-process) [12,13].

In this Letter we report the observation of a large probability of $\beta 2n$ emission from ^{86}Ga, an isotope that lies 15 neutrons away from the heaviest stable Ga and is located in the predicted r-process path [14]. The Q_β is 15.3(8) MeV and the $S_{n,2n}$ of its β daughter (^{86}Ge) are estimated to be 4.7(3) and 7.8(3) MeV, respectively [15]. This places ^{86}Ga among the best candidates for the observation of the $\beta 2n$ channel [16]. Therefore, we combined γ-ray and neutron detection systems in order to unambiguously identify this channel by observation of β-γ, β-neutron-γ, and β-neutron-neutron coincidences.

The experiment was performed at the Holifield Radioactive Ion Beam Facility (HRIBF) at Oak Ridge National Laboratory. The HRIBF [17] is an isotope separation on-line facility (ISOL), where a 50 MeV proton beam with an average intensity of 15 μA was used to induce fission in a UC_x target. Ions of ^{86}Ga were extracted from the Resonant Ionization Laser Ion Source (RILIS), utilizing a two-step ionization scheme [18], accelerated to 200 keV kinetic energy, and mass analyzed by a two-stage mass separator having mass resolving powers $M/\Delta M$ of 1000 and 10 000, respectively.

The pure ^{86}Ga beam was transmitted to the Low-Energy Radioactive Ion Beam Spectroscopy Station (LeRIBSS). We compared the γ spectra with those obtained using the electron beam plasma ion source in previous experiments

[19–21]. We did not observe any impurities for the ^{83,85,86}Ga settings of the separator when the RILIS was used. It must be noted that the key to this achievement is the selective laser ionization of Ga isotopes combined with the high-resolution electromagnetic separation. With non-optimized magnet settings, we were able to detect the presence of surface ionized atoms of ^{86}Rb^{m}, indicating that without the high resolution magnet, the superior beam purity could not have been achieved.

The LeRIBSS station was equipped with a moving tape collector (MTC), two high-purity germanium clover detectors, two plastic β detectors and 48 ^{3}He ionization chambers for neutron detection. The neutron counters, containing in total about 600 liters of ^{3}He, were mounted in a thermalizing high-density polyethylene (HDPE) support with a 1-mm-thick cadmium outer shielding. The detection of neutrons in the ^{3}He counters is based on a capture reaction; therefore, the neutron-neutron coincidences cannot be triggered by the same particle. The beam was implanted into the tape positioned at the center of the setup. The measurement cycle consisted of 2 s activity buildup, 1 s decay with no beam on, and a 0.7 s tape transport that moved the irradiated spot into a chamber located behind 5 cm of lead shielding. This cycle was continuously repeated for 19 and 48 h, for ^{86}Ga and ^{85}Ga activities, respectively.

The germanium detector efficiencies were determined with standard γ-ray calibration sources. The efficiencies of β [$\varepsilon_\beta = 50(5)\%$] and neutron counters [$\varepsilon_n = 10(2)\%$], within the 100 μs correlation window, were found from comparison between the on-line γ-ray data gated and not gated by the β and neutron detectors.

The readout of the detection system, including MTC logic signals, was based on the XIA Pixie16 Rev. F digital electronics modules [22]. The acquisition system was operated without a master trigger, and all events were recorded independently and time stamped with a 250 MHz clock synchronized across all modules. This allowed for the detailed off-line analysis of the data, including event-by-event analysis.

The β-gated and neutron-gated γ spectra for the ^{85}Ga and ^{86}Ga settings are presented in Fig. 1. The 624 keV γ ray dominating in the ^{85}Ga decay [see plot (b)] is clearly seen in all four γ spectra. This line was previously identified as the deexcitation of the first 2^+ level in ^{84}Ge [19]. Since it is detected in both ^{85}Ga and ^{86}Ga neutron-gated γ spectra, it must be emitted following $\beta 1n$ and $\beta 2n$, respectively.

The strongest line in the neutron-gated spectrum for the ^{86}Ga decay [Fig. 1(c)] is 107 keV, which has been assigned to ^{85}Ga decay [23]. This γ ray is seen in the β-gated γ spectrum of ^{85}Ga decay, but not in the neutron-gated data.

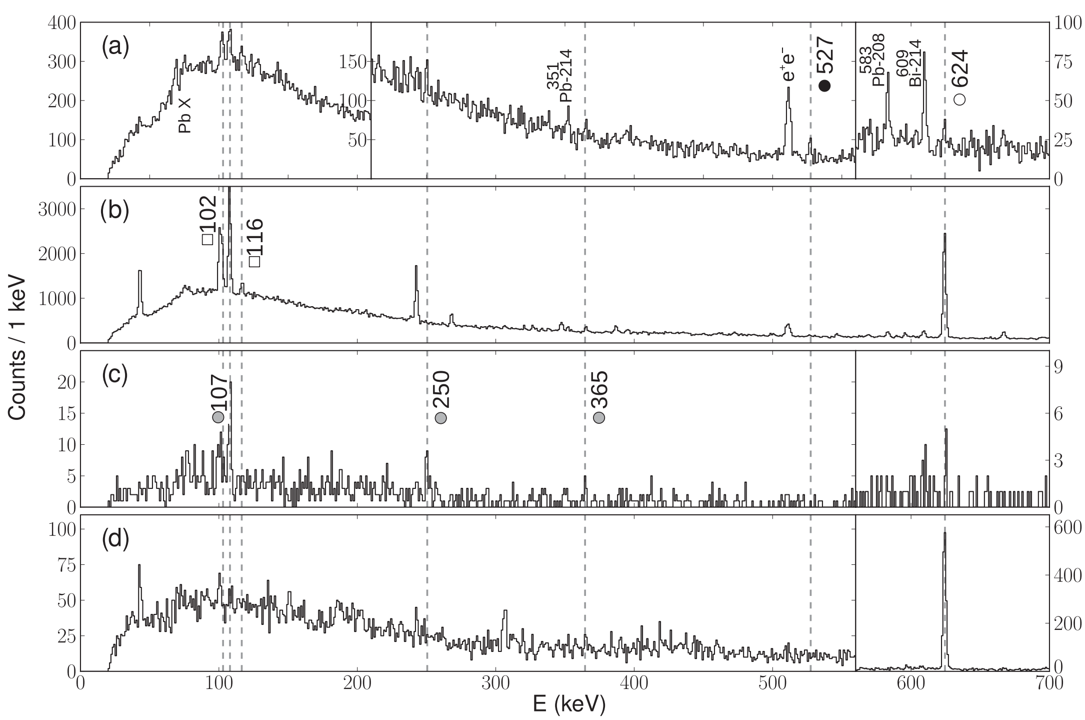

FIG. 1. (a) The low-energy part of the β-gated γ-ray spectrum for ^{86}Ga decay. Background lines are indicated by their parent activity. Other lines are marked with black circles ($\beta 0n$ ^{86}Ga $\rightarrow$ ^{86}Ge), gray circles (βn ^{86}Ga $\rightarrow$ ^{85}Ge), open circles ($\beta 2n$ ^{86}Ga $\rightarrow$ ^{84}Ge) and squares ($\beta 0n$ ^{85}Ge $\rightarrow$ ^{85}As). (b) Beta-gated γ-ray spectrum for ^{85}Ga decay. (c) Neutron-gated γ-ray spectrum for ^{86}Ga decay. (d) Neutron-gated γ-ray spectrum for ^{85}Ga decay. Note changes to the vertical scale.

Therefore, it must be a deexcitation of a state in ^{85}Ge. We see a similar relationship for the 365 keV transition. The data for the ^{85}Ga decay show a clear coincidence between 107 and 365 keV transitions. We assign the 250 keV γ ray to the $\beta 1n$-γ decay of ^{86}Ga, although it was not seen in the $\beta\gamma$ decay of ^{85}Ga. A similar situation exists in the decay of ^{83,84}Ga, where the 247 keV $1/2^+$ state was weakly populated in ^{83}Ga $\beta\gamma$ decay yet strongly populated in ^{84}Ga $\beta 1n$-γ decay [19].

The 527 keV γ ray is seen only in the β-gated γ spectrum for the ^{86}Ga activity. It is not known in the decay of other $A = 86$, 85, and 84 isotopes populated in the experiment. Therefore, we interpret this line as a transition in ^{86}Ge. Based on the energy level systematics for the even-A Ge isotopes, we assign it to the deexcitation of the first 2^+ state in ^{86}Ge. As shown in Fig. 2, the 2^+ energies in Ge exhibit the expected decrease with increasing N above the closed shell ($N = 50$), as do the observed Kr isotopes. This is in contrast to the increase in the $N = 54$ isotone ^{88}Se 2^+ energy (886 keV) observed by Jones *et al.* [24].

The decay times of the events located in the 107, 250, 365, 527, and 624 keV peaks assigned to the decay of ^{86}Ga were analyzed with the maximum likelihood method on an event-by-event basis. The likelihood function included both grow-in and decay parts of the cycle as well as the probability of background events measured near the γ peaks. We found consistent results for all five peaks. The combined result yielded $T_{1/2} = 43^{+21}_{-15}$ ms. The dependency of the maximum likelihood function on the ^{86}Ga half-life is shown in the Fig. 3(a). The probability densities of analyzed β-gated γ-ray events and events in the background gates are shown in Fig. 3(b). The same method was used for the 624 keV line following ^{85}Ga decay and resulted in $T_{1/2} = 92(4)$ ms [Fig. 3(a)], in perfect agreement with 93(7) ms from Ref. [23].

Since $\beta 2n$ decay is suggested based on the observed β-delayed neutron-gated γ-ray spectrum for ^{86}Ga neutron-neutron coincidences should be observed in the ^{3}He detector array. Figures 3(c) and 3(d) presents histograms of the β-neutron and β-neutron-neutron coincidence events versus the cycle time. It is worth noticing that all daughters and granddaughters of ^{86}Ga are β-delayed neutron emitters and contribute to the spectrum. The random background was measured on-line, during the tape movement. It was found that the irradiated spot was already inside the shielded chamber after 300 ms of tape transport. Since the β particles were stopped by the shielding, only random β-neutron coincidences, within the 100 μs time correlation window, may have been registered. We estimate that 5% of the total βn events are due to random correlations. However, the estimated probability of random $\beta 2n$ coincidences is 10^{-12}, and we did not record any $\beta 2n$ events during the background

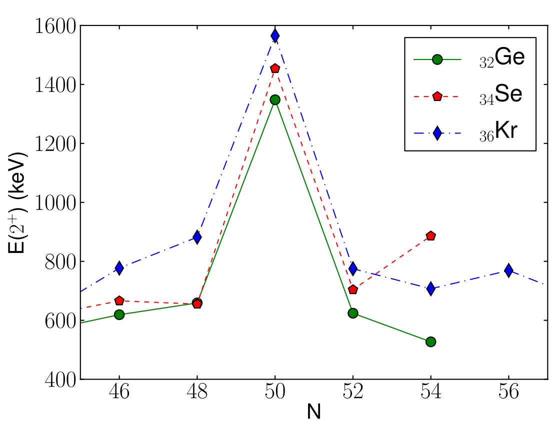

FIG. 2 (color online). Systematics of the 2_1^+ energy in the $Z = 32$–36 isotopes between $N = 46$ and 56.

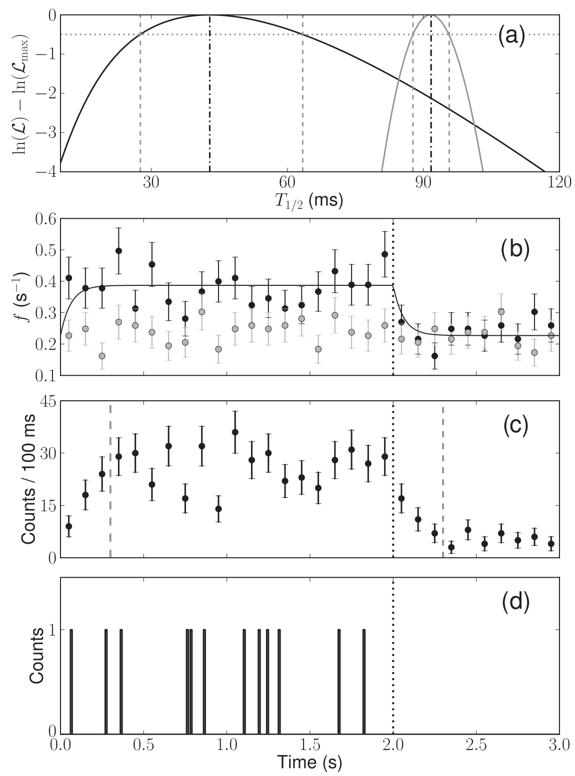

FIG. 3. (a) Maximum likelihood analysis of the ^{86}Ga (black line) and ^{85}Ga (gray line) half-lives. The dash-dotted lines show the maximum of the likelihood function. The dashed vertical lines show the 1σ limit. (b) Probability density of β-gated γ-ray events in ^{86}Ga (black points). The gray points show the distribution of events in the background gates. The black line shows the probability density function obtained with the maximum likelihood method. The start of the activity collection corresponds to the zero on the time axis, and the dotted line shows the end of the grow-in part of the cycle. (c) Histogram of the $\beta 1n$ coincidence events for the ^{86}Ga decay. The dashed lines show the gates used in the branching ratio calculations (see text for more details). (d) Time distribution of the recorded $\beta 2n$ coincidence events for the ^{86}Ga decay.

measurement. The total number of observed events was 610 β-neutron (background subtracted) and 12 β-neutron-neutron events (see Fig. 3).

In order to deduce the absolute $\beta 1n$ and $\beta 2n$ branching ratios we utilized the fact that the stopped beam contained only ^{86}Ga, and all other activities emerged as decay products. We calculated the expectation number of neutrons per ^{86}Ga ion, using a network of daughter and granddaughter activities which included isotopes of $^{84-86}$Ge, $^{83-86}$As, and $^{83-86}$Se. In this calculation, the only unknown parameters were $P_{1n}(^{86}\mathrm{Ge})$, $P_{1n}(^{86}\mathrm{Ga})$, and $P_{2n}(^{86}\mathrm{Ga})$; all half-lives and neutron branching ratios of other nuclei are known experimentally [15,20]. The unknown parameters were adjusted in 5% steps between 0% and 100%. From the calculated β-gated neutron vs time spectrum, we derived the following values: (i) the ratio of counts in the 0–0.3 s cycle period to the total number of counts; (ii) the ratio of counts in the 2.3–3.0 s period to the total number of counts; (iii) the ratio of $\beta 2n$ events to βn events. The calculated ratios included β and neutron detection efficiencies and were compared with the experimental spectra [see Figs. 3(c) and 3(d)].

We have found that only a relatively narrow subset of parameters explains the experimentally observed values. The resulting neutron emission probabilities are $P_{1n}(^{86}\mathrm{Ga}) = 60(10)\%$ and $P_{2n}(^{86}\mathrm{Ga}) = 20(10)\%$. At the same time we can give an estimate of 45(15)% for the unknown $P_{1n}(^{86}\mathrm{Ge})$. The uncertainties of the P_n values are mostly driven by a low statistics. From the comparison of the expectation number of neutrons per ^{86}Ga ion and the number of detected neutrons, we found the absolute number of implanted ions to be $13\,600 \pm 1500$. This corresponds to an implantation of about 0.3 ion/s.

From the β-gated γ spectrum we have found the absolute number of counts in the peaks assigned to the decay of ^{86}Ga. In all daughter activities we see that a significant number of decays must proceed through undetected γ transitions or directly to the ground state. The results are summarized in Fig. 4.

We have compared the $T_{1/2}$ and $P_{n,2n}$ values with the following model predictions: the FRDM + QRPA [9], the most recent version of that model FRDM + QRPA2 [10], and the microscopic spherical model based on the energy density functional DF3a with continuum quasiparticle random phase approximation (DF3a + CQRPA) [23,25]. An additional calculation was performed within the latter framework with a phenomenological fragmentation of the β-strength function included, that, to some extent, mimics the deformation of the nucleus and other higher order effects beyond the proton-neutron QRPA. The summary is presented in Table I.

Except for the older FRDM + QRPA the models overpredict the half-life and the P_{2n}/P_{1n} ratio. In the case of the FRDM + QRPA2 model the authors assumed a spherical shape for the $^{83-87}$Ga isotopes [26]. However, for the first

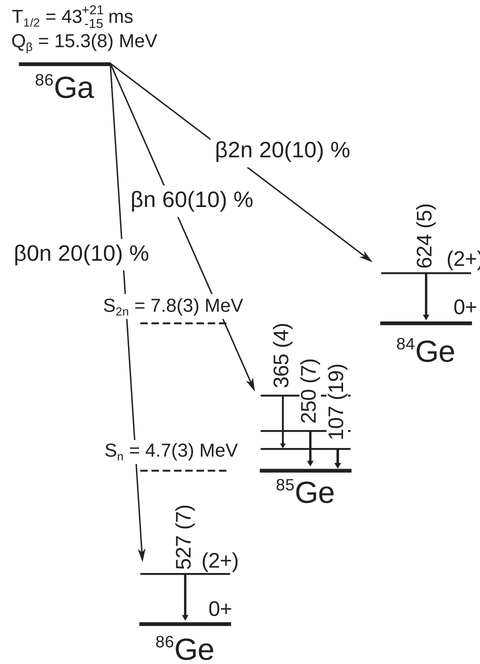

FIG. 4. The proposed decay scheme of ^{86}Ga (not drawn to scale). The γ transitions are identified by energy in keV, the intensities, given in parenthesis, are normalized per 100 ^{86}Ga decays. The Q_β and $S_{n,2n}$ values are from [15]. Other values are from this work.

2^+ state in ^{86}Ge located at 527 keV, we get a deformation parameter of $\beta_2 = 0.24(2)$ using Raman's empirical estimate [27]. The FRDM model yields $\beta_2 = 0.17$ [9] for ^{86}Ge, also suggesting the onset of deformation. The inclusion of fragmentation of the β strength in the DF3a + CQRPA model improved the agreement with the experimental result, supporting the need to include the deformation.

Both models use a microscopic approach to obtain the β-strength function. The subsequent deexcitation is based on a simple assumption that the levels fed in β-decay located within the $S_{2n} - S_n$ window decay by $1n$ emission, and within the $Q_\beta - S_{2n}$ window by $2n$ emission. However, the large excitation energy of the daughter nucleus is expected to result in a high level density and strong mixing of the configurations that open multiple, highly fragmented, paths of decay. In order to provide more

TABLE I. Comparison of the experimental results and predictions of ^{86}Ga half-life and β-delayed emission probabilities of theoretical models used in the astrophysical calculations.

Model	$T_{1/2}$ (ms)	P_{1n} (%)	P_{2n} (%)
Experiment	43^{+21}_{-15}	60(10)	20(10)
FRDM + QRPA	26	61	13
FRDM + QRPA2	128	20	44
DF3a + CQRPA	86	20	12
DF3a + CQRPA + frag.	68	28	22

realistic branching ratio estimates, an improved model should take into account the statistical nature of the deexcitation process governed by the competition between the γ rays, $\beta 1n$, and $\beta 2n$ emissions throughout the entire Q_β window.

In summary, we report the first observation of ^{86}Ga β decay, its half-life, and absolute P_{1n} and P_{2n} values. In addition, the (2^+) state in ^{86}Ge was identified. The experiment was made possible with a pure beam of ^{86}Ga that was achieved through laser ionization and high-resolution electromagnetic separation. The $\beta 2n$ decay branch is unambiguously identified by β-neutron-neutron correlations and by observation of the 624 keV transition in ^{84}Ge. We observed for the first time a large $\beta 2n$ branch in a fission fragment nucleus. These results are of importance for guiding the development of nuclear structure and β-decay models, as well as in the simulation of the r-process and its resulting mass abundances. The results confirm the theoretical predictions of significant $\beta 2n$ probability in the decay of ^{86}Ga, and they suggest that the onset of deformation and the competition between $1n$ and $2n$ emission are important factors in the predictions of the half-life and delayed neutron branches of neutron-rich nuclei.

We would like to thank the HRIBF operations staff for the production of excellent radioactive ion beams. K. Miernik's research was performed as a Eugene P. Wigner Fellow and staff member at the Oak Ridge National Laboratory, managed by UT-Battelle, LLC, for the U.S. Department of Energy under Contract DE-AC05-00OR22725. This research is sponsored by the Office of Nuclear Physics, U.S. Department of Energy under Contracts No. DE-AC05-00OR22725 (ORNL), No. DE-FG02-96ER41006(MSU), No. DE-FG02-96ER40983 (UTK), and No. DE-AC05-06OR23100(ORAU). The authors from the University of Warsaw acknowledge the support of National Science Center of the Polish Ministry of Science and Higher Education, Grant No. 2011/01/B/ST2/02476. I. B. is partially supported by Helmholtz Alliance EMMI and the Grant by IN2P3-RFBR under Agreement No. 110291054. This research was sponsored in part by the National Nuclear Security Administration under the Stewardship Science Academic Alliances program through DOE Cooperative Agreement No. DE-FG52-08NA28552.

*krzysztof.miernik@fuw.edu.pl

[1] R. Roberts, R. Meyer, and P. Wang, Phys. Rev. **55**, 510 (1939).
[2] N. Bohr and J. Wheeler, Phys. Rev. **56**, 426 (1939).
[3] V. Goldansky, Nucl. Phys. **19**, 482 (1960).
[4] R. Azuma *et al.*, Phys. Rev. Lett. **43**, 1652 (1979).
[5] M. Borge, Phys. Scr. **T152**, 014013 (2013).
[6] K. Yoneda *et al.*, Phys. Rev. C **67**, 014316 (2003).
[7] P. Reeder, R. Warner, T. Yeh, R. Chrien, R. Gill, M. Shmid, H. Liou, and M. Stelts, Phys. Rev. Lett. **47**, 483 (1981).
[8] B. Jonson *et al.*, *Proceedings of the 4th International Conference on Nuclei Far From Stability, Helsingør, 1981*, CERN Report No. CERN-81-09 (CERN-Service d'information scientifique, Geneva, 1981), p. 265.
[9] P. Möller, J. Nix, and K.-L. Kratz, At. Data Nucl. Data Tables **66**, 131 (1997).
[10] P. Möller, B. Pfeiffer, and K.-L. Kratz, Phys. Rev. C **67**, 055802 (2003).
[11] D. Abriola, B. Singh, and I. Dillman, IAEA International Nuclear Data Committee I NDC(NDS)-0599 (2011).
[12] G. Wallerstein *et al.*, Rev. Mod. Phys. **69**, 995 (1997).
[13] M. R. Mumpower, G. C. McLaughlin, and R. Surman, Astrophys. J. **752**, 117 (2012).
[14] K.-L. Kratz, AIP Conf. Proc. **819**, 409 (2006).
[15] M. Wang, G. Audi, A. H. Wapstra, F. G. Kondev, M. MacCormick, X. Xu, and B. Pfeiffer, Chinese Phys. C **36**, 1603 (2012).
[16] P. Möller, http://t2.lanl.gov/nis/molleretal/publications/rspeed2002.html.
[17] J. Beene, D. W. Bardayan, A. G. Uribarri, C. J. Gross, K. L. Jones, J. F. Liang, W. Nazarewicz, D. W. Stracener, B. A. Tatum, and R. L. Varner, J. Phys. G **38**, 024002 (2011).
[18] Y. Liu *et al.*, Nucl. Instrum. Methods Phys. Res., Sect. B **298**, 5 (2013).
[19] J. Winger *et al.*, Phys. Rev. C **81**, 044303 (2010).
[20] C. Mazzocchi *et al.*, Phys. Rev. C **87**, 034315 (2013).
[21] A. Korgul *et al.* (to be published).
[22] http://www.xia.com/.
[23] M. Madurga *et al.*, Phys. Rev. Lett. **109**, 112501 (2012).
[24] E. Jones *et al.*, Phys. Rev. C **73**, 017301 (2006).
[25] I. N. Borzov, Phys. Rev. C **67**, 025802 (2003).
[26] B. Pfeiffer, K.-L. Kratz, and P. Möller, Prog. Nucl. Energy **41**, 39 (2002).
[27] S. Raman, C. Nestor, and P. Tikkanen, At. Data Nucl. Data Tables **78**, 1 (2001).